Effects of non-condensable gas on cavitating flow over a cylinder

Filipe Brandao; Mrugank Bhatt; Krishnan Mahesh*

University of Minnesota, Minneapolis, MN, USA

Abstract

The effect of non-condensable gas in cavitating flow over a circular cylinder is investigated using a homogeneous mixture model. The numerical method to simulate turbulent cavitating flows developed by Gnanaskandan and Mahesh [1] for the mixture of water and vapor is extended to include the effect of non-condensable gas. The damping effects due to the presence of gas in the mixture are discussed. Finally, distribution of gas and vapor in the near wake of cylinder is investigated.

Keywords: non-condesable gas; cylinder; cavitation.

1. Introduction

Non-condensable gases (*NCG*) can behave differently from vapor in response to pressure variations as vapor can condense into liquid other than changing its volume. Presence of non-condensable gas can damp the collapse of vapor bubbles [2] and can decrease the condensation process at cavity interface leading to a higher bubble rebound [3]. The effects of injecting gas have been studied experimentally in context of sheet to cloud cavitation [4, 5]. Injection of a large amount of gas in the vapor cavity has been shown to prevent rapid collapse of vapor cloud thereby reducing the noise induced in the cloud cavitation [4]. Numerical methods based on incompressible Navier-Stokes equations have been developed to include the effect of non-condensable gas for studying ventilated supercavitation [6, 7, 8] as well as unsteady sheet cavitation [9]. In the present work, we extend the numerical method of Gnanskandan and Mahesh [1] based on a fully compressible formulation to account for non-condensable gas and study its effects on cavitating flow over a circular cylinder.

The paper is organized as follows. Section 2 discusses the extension of numerical method to account for non-condensable gas. Damping effect due to the presence of gas and distribution of gas and vapor in the near wake of the cylinder is discussed in section 3 and compared to the results obtained for the water-vapor mixture [10]. Finally, results are summarized in section 4.

2. Physical model and numerical method

Gnanaskandan and Mahesh [1] developed a numerical method to solve turbulent cavitating flows using a homogeneous mixture model for the mixture of water and vapor. Here, we extend this approach by introducing a non-condensable gas as a component of the homogeneous mixture in addition to vapor and water. This water-vapor-gas mixture is now treated as a single compressible fluid with thermal and mechanical equilibrium between phases. Compressible Navier-Stokes equations are solved for the mixture quantities along with transport equations for vapor and non-condensable gas. The system is closed by a mixture equation of state obtained from the stiffened equation of state for water and an ideal gas equation of state for both vapor and gas. The equation is given by

$$p = \rho T\left(Y_v R_v + Y_g R_g\right) + \left(1 - Y_v - Y_g\right)\rho K_l T \frac{p}{p + P_c} \tag{1}$$

Here, Y_v and Y_g are mass fractions for vapor and gas respectively. $R_v = 461.6\ \mathrm{J/(Kg\ K)}$, $R_g = 286.9\ \mathrm{J/(Kg\ K)}$, $K_l = 2684.075\ \mathrm{J/(Kg\ K)}$ and $P_c = 786.333 * 10^6\ \mathrm{Pa}$ are the constants associated with equation of state for vapor, gas and liquid. The expression for speed of sound in this mixture is obtained from the mixture equation of state (1) and Gibbs equation, given by

*Corresponding Author, Krishnan Mahesh: kmahesh@umn.edu

$$a^2 = \frac{C_1 T}{C_0 - C_1/C_{pm}} \tag{2}$$
$$C_1 = (Y_v R_v + Y_g R_g)(p + P_c) + (1 - Y_v - Y_g) K_l p$$
$$C_0 = 2p + P_c - \rho T(Y_v R_v + Y_g R_g) - (1 - Y_v - Y_g)\rho K_l T$$
$$C_{pm} = Y_v C_{pv} + Y_g C_{pg} + (1 - Y_v - Y_g) C_{pl}$$

Here, C_{pv}, C_{pg} and C_{pl} are specific heats at constant pressure for vapor, gas and liquid respectively. Speed of sound obtained from equation 2 for water-vapor-air mixture is plotted as a function of vapor and gas volume fraction in Figure 1(a) and compared to the experimentally available data for water-gas mixture as shown in Figure 1(b). Note that introduction of gas leads to reduction in the sound speed of mixture.

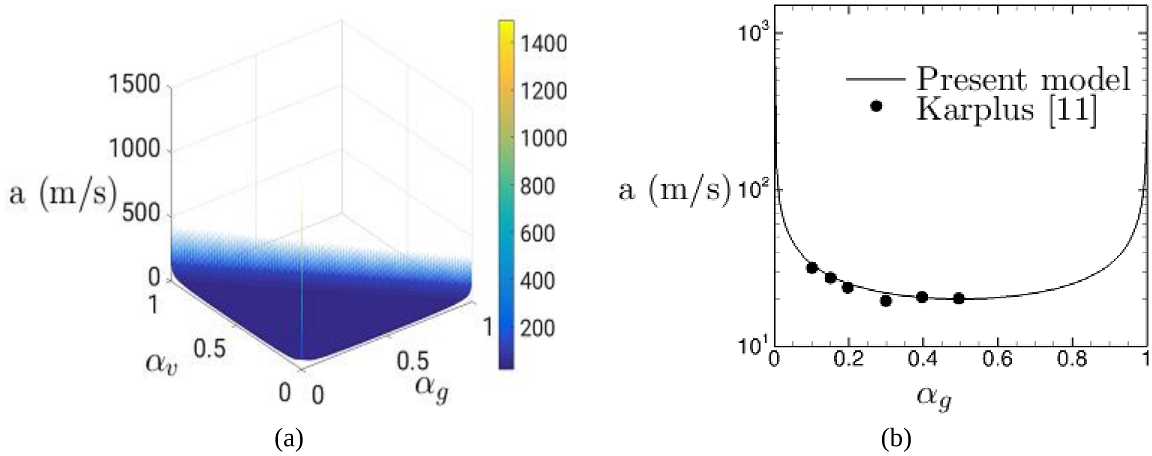

Figure 1. Speed of sound in water-vapor-gas mixture.

The numerical method is based on a predictor-corrector approach. The predictor step uses a non-dissipative scheme and corrector step applies a characteristic based filter locally in the vicinity of discontinuities. The additional equation due to the transport of non-condensable gas is coupled through Jacobians to the compressible Navier-Stokes equations, and transport equation for vapor mass fraction.

3. Results and discussion

Cavitating flow over a circular cylinder is studied at $Re = 200$ and two different cavitation numbers ($\sigma = 1.0$ and $\sigma = 0.5$). Non-condensable gas is introduced in the free stream similar to the addition of vapor nuclei in the flow. Results presented in section 3.1 correspond to $\sigma = 1.0$. Section 3.2 shows results for both $\sigma = 1.0$ and $\sigma = 0.5$.

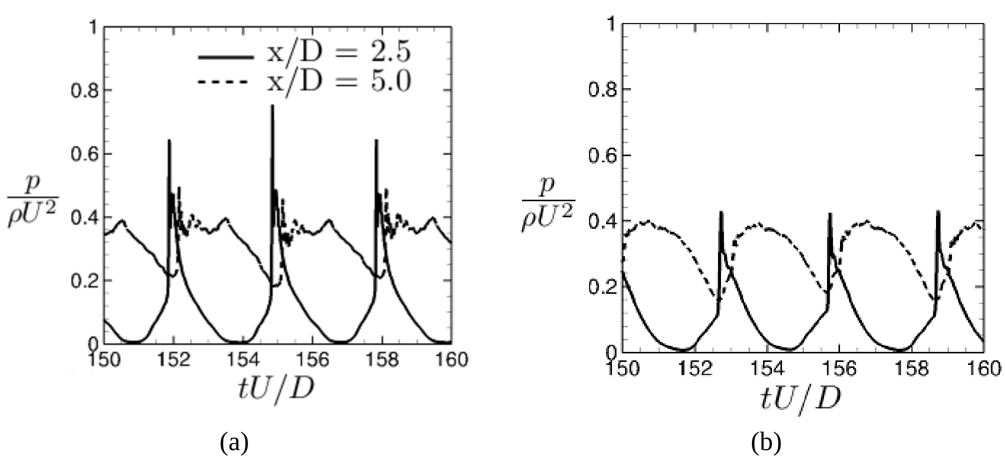

Figure 2. Pressure history for the flow where *NCG* is absent (a) and present (b).

*Corresponding Author, Krishnan Mahesh: kmahesh@umn.edu

3.1. Damping effects of gas

In order to understand the effect of gas on the pressure waves produced due to cavity collapse, we plot pressure history in the wake of cylinder at 2.5*D* and 5*D* along the wake center-line, as shown in the Figure 2 (for both flows- in presence and absence of gas). Note that at 2.5*D*, the peak value of pressure is less when the gas is present. Also, the pressure wave produced due to collapse no longer has a sharp pressure peak as it reaches the station at 5*D* as seen in Figure 2(b). The distance between the peaks at 2.5*D* and 5*D* in the time domain reflects the propagation speed of the wave, which is smaller when the gas is present. This is due to the reduction in sound speed of the mixture in the presence of gas. Smaller amplitudes of pressure waves can be explained from the inviscid, isentropic relation for pressure perturbation in the medium,

$$p - \bar{p} = \bar{a}^2(\rho - \bar{\rho}) = Z\bar{a}S \qquad (3)$$

where $S = (\rho - \bar{\rho})/\bar{\rho}$ is condensation ratio, $\bar{a}$ is sound speed and $Z = \bar{\rho}\bar{a}$ is acoustic impedance of the medium. Acoustic impedance is smaller for the medium when gas is present due to reduction in mean density and sound speed. Pressure perturbation scaled by $Z\bar{a}$ is plotted in Figure 3(a). Peak values of scaled pressure perturbations are smaller when the gas is present indicating smaller condensation ratio. This is also seen from the total void fraction plots in Figure 3(b). We can see that as the pressure wave passes through the medium in which the gas is present, it creates smaller drop in total gaseous phase void fraction. Reduction in sound speed, lower acoustic impedance and smaller condensation ratio entails smaller pressure perturbation in the presence of non-condensable gas as seen from equation 3. Therefore, in the presence of gas weaker pressure waves impinge on the cylinder surface. Consequently, the secondary peak in lift curve, which is due to the impingement of the pressure wave on the cylinder surface (primary peak correspond to cavity shedding) as shown in Figure 3(c), is absent in the presence of non-condensable gas.

Figure 4 shows the root mean square of density fluctuations compared for the two cases (in presence and absence of gas). It can be observed that the density fluctuations, at the cylinder surface and in the cavity closure region, are smaller in the presence of gas. This is due to the fact that the gas does not undergo any phase change (evaporation and condensation). Consequently, the flow in presence of gas is not subject to rapid changes in density compared to the flow containing vapor alone, having a stabilizing effect on the cavity being formed.

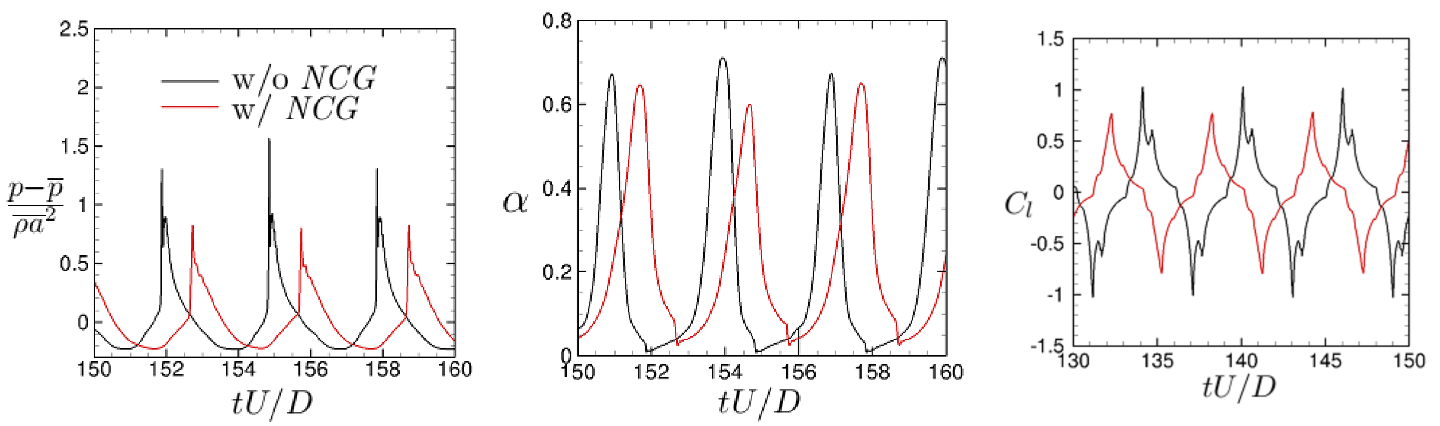

(a) (b) (c)

Figure 3. Scaled pressure pertubation (a) and total void fraction (b) along the wake centerline at *x/D* = 2.5 and lift curves (c).

*Corresponding Author, Krishnan Mahesh: kmahesh@umn.edu

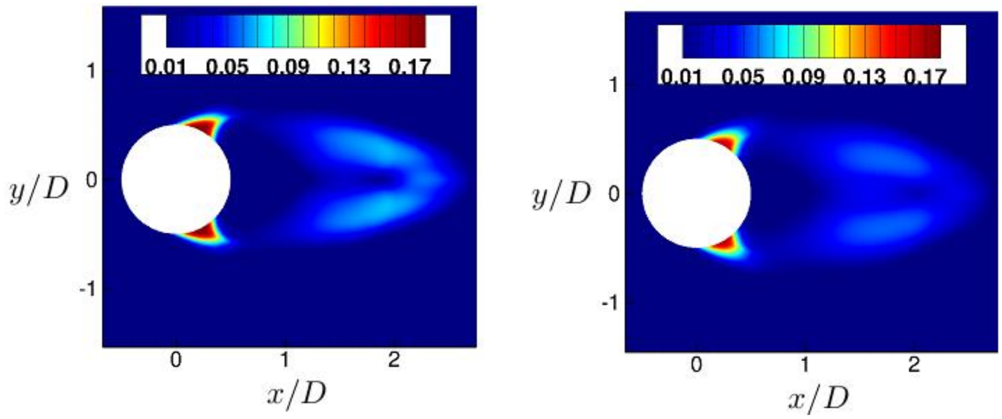

(a) (b)

Figure 4. Density fluctuation contour for the flow where *NCG* is absent (a) and present (b).

3.2. Near wake profiles of vapor and gas

Non-condensable gas can behave differently from vapor particularly in the regions of flow which are susceptible to phase change. First, consider $\sigma = 1.0$ (higher cavitation number). Figure 5(a,b) shows evolution of gas and vapor volume fraction with time at 2.5D and 5D on wake centerline. Note that the volume fraction of vapor is higher than the volume fraction of *NCG* in the region close to the cylinder at 2.5D, where evaporation is taking place. However, for the positions further downstream at 5D in the region of pressure recovery both are nearly same and close to the free stream values.

Next, we present the void fraction profiles when the cavitation number in the free stream is reduced ($\sigma = 0.5$). Figure 6(a,b) shows void fraction contours of vapor and gas respectively in the wake of cylinder at an instant when the cavity is fully attached to the body. Higher gas void fractions are observed in the shear layer and the aft portion of cavity as seen from Figure 6(b), whereas vapor is concentrated in the regions in the rear part of the cylinder as in Figure 6(a). This can be explained from the void fraction profiles taken radially on the cylinder surface as shown in Figure 6(c) at 2 different azimuthal location. For $\theta = 70°$ we see that there is no difference in gas and vapor volume fraction, also their magnitude is small since flow mostly consist of water. The distribution at $\theta = 130°$ where cavity is being formed on cylinder surface, shows that volume fraction of vapor is maximum near the surface due to the production of vapor when the pressure drops below vapor pressure. It is also noticeable that gas volume fraction is maximum in the shear layer and not at the surface of cylinder. Thus, this region of high *NCG* concentration is convected downstream when the cavity grows giving rise to the "wing" shape observed in Figure 6(b).

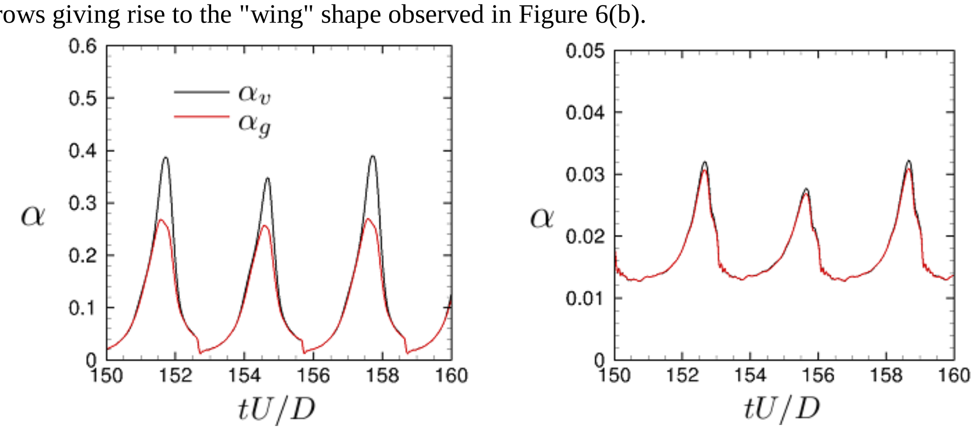

(a) (b)

Figure 5. Time history of vapor (black) and *NCG* (red) volume fraction at two different locations along the wake centerline: (a) *x/D* = 2.5, (b) *x/D* = 5.0.

*Corresponding Author, Krishnan Mahesh: kmahesh@umn.edu

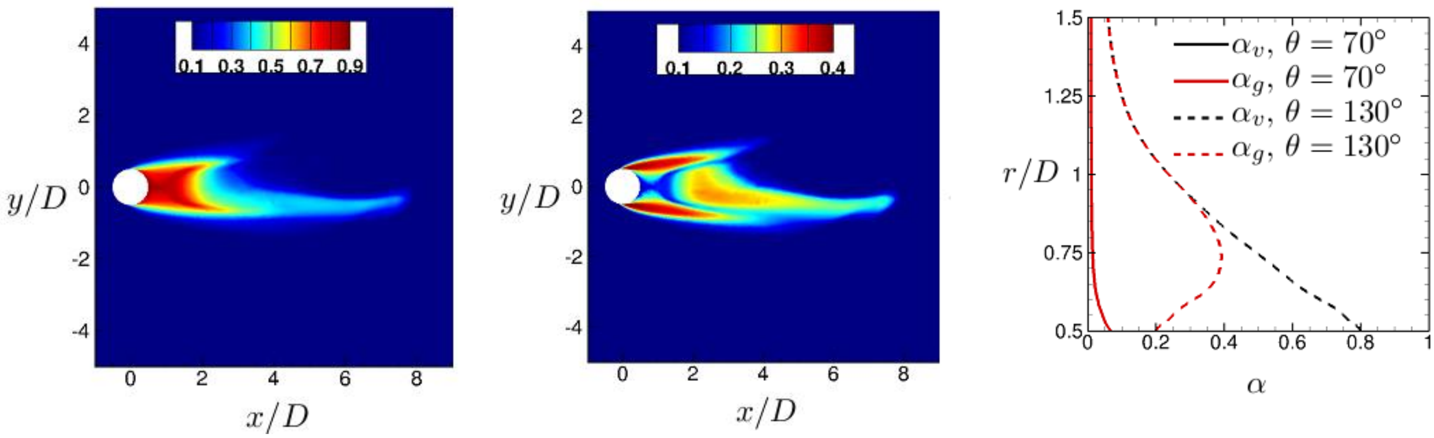

(a) (b) (c)

Figure 6. Volume fraction of vapor (a) and *NCG* (b) when the cavity is fully attached to the cylinder. Radial void fraction profiles of vapor and *NCG* at the cylinder surface (c).

4. Summary

A numerical method to simulate turbulent cavitating flows developed for the water-vapor mixture has been extended to include the effects of non-condensable gas. The speed of sound for the water-vapor-gas mixture shows good agreement with experimental data. Cavitating flow over a circular cylinder in the presence of non-condensable gas is studied at different free stream cavitation numbers. Damping of pressure perturbations due to the presence of gas in the medium is discussed. Vapor and gas uniformly introduced in the free stream, distribute themselves differently in the wake of cylinder depending upon the local flow conditions.

Acknowledgments

This work is supported by the United States Office of Naval Research under Grant ONR N00014-17-1-2676 with Dr. Ki-Han Kim as the program manager. Computing resources were provided by the Minnesota Supercomputing Institute (MSI).

References

[1] Gnanaskandan, A. and Mahesh, K. (2015). *A numerical method to simulate turbulent cavitating fows*. International Journal of Multiphase Flows 70 22-34.

[2] Franc, J-P. (2006). *Physics and Control of Cavitation*. In: Design and Analysis of High Speed Pumps. Educational Notes RTO-EN-AVT-143 2-1 - 2-36.

[3] Akhatov, I., Lindau, O., Topolnikov, A., Mettin, R., Vakhitova, N., Lauterborn, W. (2001). *Collapse and rebound of a laser-induced cavitation bubble*. Physics of Fluids 13(10).

[4] Reisman, G., Duttweiler, M., Brennen, C. (1997). *Effect of Air Injection on the Cloud Cavitation of a Hydrofoil*. ASME Fluids Engineering Division Summer Meeting.

[5] Makiharju, SA., Ganesh, H. Ceccio, SL. (2015). *Effect of non-condensable gas injection on cavitation dynamics of partial cavities*. Journal of Physics: Conference Series 656

[6] Kunz, R., Boger, F., Stinebring, D.R., Chyczewski, T.S., Lindau, J.W., Gibeling, H.J., Venkateswaran, S., Govindan, T.R. (2000). *A preconditioned Navier-Stokes method for two-phase flows with application to cavitation*. Computers and Fluids, 29(8), pp. 849-875.

[7] Singhal, A.K., Athavale M.M., Li H., Jiang Y. (2002). *Mathematical basis and validation of the full cavitation model*. Journal of Fluids Engineering, 124, pp. 617-624.

[8] Ji, B., Luo, X., Peng, X., Zhang, Y., Wu, Y.,Xu, H. (2010). *Numerical investigation of the ventilated cavitating flow around an under-water vehicle based on a three-component cavitation model*. Journal of Hydrodynamics, 22(6), pp. 753-759.

[9] Lu, N-X., Bark, G., Bensow, R. (2012). *Introducing Non-condensable Gas in Unsteady Sheet Cavitation Modelling*. 15th Numerical Towing Tank Symposium.

*Corresponding Author, Krishnan Mahesh: kmahesh@umn.edu

[10] Gnanaskandan, A. and Mahesh, K. (2016). *Numerical investigation of near-wake characteristics of cavitating flow over a circular cylinder*. Journal of Fluid Mechanics 790 453-491.
[11] Karplus, H. B. (1957). *Velocity of sound in a liquid containing gas bubbles*. The Journal of Acoustical Society of America 29 12-61.

*Corresponding Author, Krishnan Mahesh: kmahesh@umn.edu